PAPER

Metal-free activation of H_2O_2 by g-C_3N_4 under visible light irradiation for the degradation of organic pollutants†

Yanjuan Cui,[a] **Zhengxin Ding,**[a] **Ping Liu,**[a] **Markus Antonietti,**[b] **Xianzhi Fu**[a] **and Xinchen Wang*[a]**

Semiconducting carbon nitride materials were successfully prepared *via* a thermal poly-condensation of dicyandiamide as a precursor at > 500 °C. The resulting materials were investigated as metal-free catalysts for the activation of H_2O_2 with visible light under mild conditions, using the decomposition of Rhodamine B (RhB) in aqueous solution as a model reaction. Results revealed that carbon nitride catalysts can activate H_2O_2 to generate reactive oxy-radicals under visible light irradiation without employment of any metal additives, leading to the mineralization of the dye. Factors affecting the degradation of organic compounds are pH values and the concentration of H_2O_2. Recycling of the catalyst indicated no obvious deactivation during the entire catalytic reaction, indicating good (photo)chemical stability of metal-free polymeric carbon nitride photocatalysts for environmental purification. This study demonstrated a promising approach for the activation of green oxidant, hydrogen peroxide, by the newly-developed polymer photocatalysts for environmental remediation and oxidation catalysis.

1. Introduction

Organic dyes are widely used in a variety of technical applications, including dyeing of textiles, paper, plastics, or leather. Due to their (partial) toxicity, mutagenicity and carcinogenicity, a simple way to remove organic dyes from industrial wastewater, especially in developing countries, is recognized as an urgent challenge. Most of the dye molecules are found to be resistant against normal biodegradation under aerobic conditions, while the use of anaerobic degradation produces carcinogenic products, such as aromatic amines, as breakdown products. The development of cost-efficient and environmentally benign approaches for the removal of synthetic dyes from wastewater is therefore still a very active and ecologically important issue.

Various advanced oxidative processes (AOPs) have been investigated for the degradation of organic dyes in water, including UV/H_2O_2,[1] Fenton/photo-Fenton schemes,[2] electrochemical catalysis,[3] and semiconductor photocatalysis.[4] Among the latter, TiO_2 has been investigated primarily, as this catalyst enables the *in situ* generation of strong oxidizing intermediates from clean sources such as oxygen or hydrogen

peroxide to degrade even rather persistent pollutants under relatively mild conditions. However, due to its rather wide band gap (3.2 eV) the application of TiO_2 is limited to UV light, which makes up only ~4% of the incoming solar energy on the Earth. Great efforts have consequently been devoted to narrowing the band gap of TiO_2 by chemical modifications, and concurrently the search for new photocatalysts capable of working within the visible light range is still going on.

H_2O_2 is one of the used green oxidants, relevant for organic synthesis[5] and in the present context for water purification. Usually, in both cases a catalyst is typically required to activate H_2O_2 to produce more reactive oxidizing intermediates. Photo-Fenton agents (Fe^{2+}, Fe^{3+}/H_2O_2) have been extensively applied to decompose H_2O_2 to the hydroxyl radical ($^\bullet$OH), but this process is restricted to low pH (typically < 3) and suffers from difficulties of follow-up product separation. Heterogeneous solid Fenton-like catalysts, such as Fe^0/FeO_xH_{2x-3}, Fe_2O_3/SiO_2 and $FePZ(dtnCl_2)_4$, were therefore developed to replace homogeneous catalysts.[6–8] Non-ferrous catalysts have also been explored as activation catalysts for H_2O_2, for example, copper-pillared clays (Cu-PILC) were reported to decompose organic waste using H_2O_2.[9] A chromate(III)/H_2O_2 system was demonstrated to be most effective in the oxidative degradation of organic pollutants over a wide pH range (*i.e.* pH = 3–11),[10] but suffers from being itself an even stronger pollutant. Therefore, we consider a metal-free catalyst that is capable of activating H_2O_2 under mild conditions as an interesting alternative not only for catalytic synthesis but also for environmental purification.
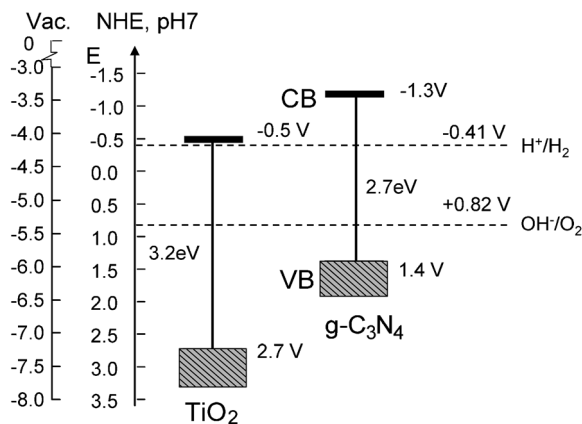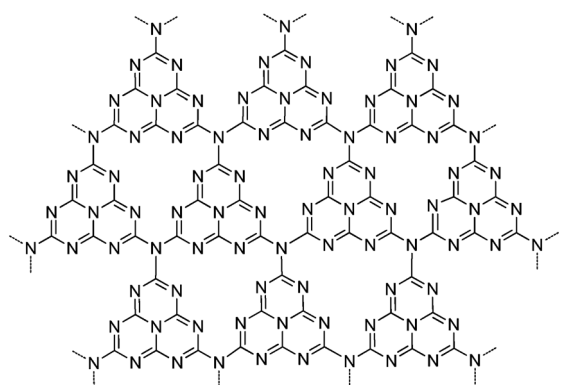
[a] *Research Institute of Photocatalysis, State Key Laboratory Breeding Base of Photocatalysis, Fuzhou University, Fuzhou 350002, People's Republic of China. E-mail: xcwang@fzu.edu.cn; Fax: +86-591-83738608; Tel: +86-591-83779326*
[b] *Max-Planck Institute of Colloids and Interfaces, Department of Colloid Chemistry, Research Campus Golm, 14424 Potsdam, Germany*
† Electronic supplementary information (ESI) available: More characterization and reaction results. See DOI: 10.1039/c1cp22820j

Recently, covalent carbon nitride-based solids have attracted widespread interest in a variety of catalytic applications.[11] A slightly disordered, graphitic carbon nitride (termed as g-C_3N_4) was found to be a stable, metal-free photocatalyst working with visible light (Scheme 1). This material can be synthesized via bulk condensation of appropriate nitrogen-rich precursors, such as cyanamide, dicyandiamide, or melamine. The covalent solid possesses a band gap of 2.7 eV, with appropriate positions of the conduction band (CB) and valence band (VB) [CB = −1.3 V, VB = 1.4 V vs. NHE, pH = 7][12] to run a set of relevant activation reactions (Scheme 1). For instance, g-C_3N_4 was able to split photochemically water into hydrogen or oxygen in the presence of an electron donor or acceptor,[13] but can also activate H_2O_2 for the direct oxidation of benzene to phenol.[14] An iron-doped g-C_3N_4 has been used to decompose H_2O_2 to •OH for mineralizing organic dyes like Rhodamine B (RhB) to CO_2.[15] Yan et al. recently reported the photocatalytic performance of g-C_3N_4 synthesized by direct heating of melamine.[16] Their results confirmed its potential to degrade organic dyes without noticeable deactivation throughout the reaction, but in the given examples only with moderate activity. And the reactive species and reaction intermediates during the photocatalytic process have yet to be explored.

In this article, we report on the advancement of carbon nitride photocatalysts for environmental application. g-C_3N_4 was synthesized from dicyandiamide,[17] and the photocatalytic properties of g-C_3N_4 were evaluated via the decomposition of Rhodamine B in aqueous solution. The reactive species during the photocatalytic activation of H_2O_2 by g-C_3N_4 was examined, and the photodegradation mechanism is also discussed.

2. Experimental

2.1. Materials

Dicyandiamide (99%), 5,5′-dimethylpyrroline-N-oxide (DMPO) and Rhodamine B (tetraethyl-rhodamine (RhB)), analytical grade, were purchased from Sigma Aldrich Chemical Co. and used without further purification. H_2O_2 (30%, w/w) was provided by Sinopharm Chemical Reagent Co., Ltd. (Shanghai, China).

2.2. Preparation of catalysts

g-C_3N_4 was prepared by thermal polycondensation of dicyandiamide according to the reported procedure.[18] In a typical synthesis, 10 g dicyandiamide was put into a crucible with a cover and calcined at settled temperatures for 4 h in a muffle furnace, using a heating rate of 2.3 °C min^{-1}. The sample was then allowed to cool to room temperature before removal from the furnace. Yellow products were obtained after this polycondensation step. Products were denoted as CN_{450}, CN_{500}, CN_{550} and CN_{600} where the number denotes the condensation temperature.

2.3. Photocatalytic tests

A 500 W halogen lamp was placed in a cylindrical glass vessel with a glass jacket. One pair of combined cutoff filters was placed outside the jacket to remove wavelengths below 420 nm and above 800 nm to a large extent (Fig. S1, ESI†), thereby ensuring predominant illumination with visible light with a stable optical energy flux of about 36 mW cm^{-2}. In a Pyrex glass photoreactor, 80 mL RhB solution and 40 mg catalyst were mixed. After reaching the adsorption/desorption equilibrium within 0.5 h (Table S1, ESI†, important for monitoring an unaffected dye conversion), the lamp was turned on to initiate the photocatalytic reaction. 3 mL of the suspension were sampled at fixed time intervals during the reaction. The suspension was centrifuged to sediment the catalyst and then analyzed by UV-Vis spectroscopy using a Cary 50 UV-Vis spectrophotometer. The different pH values of the photocatalytic experiments were adjusted by using HCl and/or NaOH aqueous solutions.

2.4. Chemical analysis

X-Ray diffraction (XRD) patterns were collected using a Bruker D8 Advance X-ray diffractometer (Cu K$_{\alpha 1}$ irradiation, λ = 1.5406 Å). A Varian Cary 500 Scan UV-Vis spectrophotometer was used to record the UV-Vis diffuse reflectance spectra of different samples with barium sulfate as the reference sample. Fourier transformed infrared (FTIR) spectra were recorded using a Nicolet Magna 670 FTIR spectrometer in KBr at a concentration of ca. 1 wt%. The photoluminescence (PL) emission spectra were taken on a FS/FL920 time-resolved fluorescence spectrometer. Liquid chromatography/mass

Scheme 1 The chemical structure of graphitic carbon nitride sheets, and the band gap structure comparison of g-C_3N_4 with titanium dioxide (TiO_2), a reference photocatalyst.

spectrometry (LCMS) was exploited to identify the intermediates of RhB during the photodegradation. The LCMS system was equipped with a Zorbax C18 column (150 mm 4.6 mm i.d. = 5 μm) and coupled on-line to an LC/MSD Trap XCT ion-trap mass spectrometer (Agilent Technologies, CA, USA). Electron spin resonance (ESR) spectra were recorded as follows. Signals of radicals spin trapped by 5,5-dimethyl-1-pyrroline-N-oxide (DMPO) were obtained using a Bruker model ESP 300E electron paramagnetic resonance spectrometer equipped with a xenon lamp (with 420 nm filter) as the light source. The total organic carbon (TOC) values were determined using a Shimadzu TOC-Vcph total organic carbon analyzer. To reduce the measurement error, the initial concentrations of RhB and catalyst were increased to 100 ppm and 5 g L^{-1}, respectively.

3. Results and discussion

3.1. Characterization

X-Ray diffraction (XRD) patterns of the g-C$_3$N$_4$ catalysts prepared at different temperatures presented a strong peak at 27.4°, characteristic of the stacking peak of pi-conjugated layers and indexed for graphitic materials as the (002) peak (Fig. 1a).[19]

It can be seen that the lowest preparation temperature of 450 °C is not sufficient to obtain fully condensed g-C$_3$N$_4$. At higher preparation temperatures of 500 and 550 °C, the intensity of the (002) peak remarkably increases, while at 600 °C the relative intensity reduces again, which points to the beginning of thermal decomposition, the formation of defects in the sample and the disturbance of the graphitic structure.

FTIR spectroscopy supports the existence of a graphite-like structure of carbon nitride, as shown in Fig. 1b. The broad absorption band at 3100–3300 cm^{-1} can be assigned to the stretching modes of secondary and primary amines and their intermolecular hydrogen-bonding interactions.[20] The band at 810 cm^{-1} belongs to s-triazine ring modes and bands at 1200–1600 cm^{-1} are characteristic of aromatic carbon nitride heterocycles.[21]

The typical UV-Vis absorption spectra of a semiconductor, with an onset of absorption at 470 nm, were observed for the samples synthesized at > 550 °C, consistent with the reported results (Fig. 1c).[13] Note that CN$_{600}$ exhibits a higher light-trapping effect in the 450–550 nm region compared to CN$_{550}$, believed to be due to carbon–carbon bonds within the CN$_{600}$ structure.

3.2. Photocatalytic performance

The photocatalytic performance of g-C$_3$N$_4$ calcinated at different temperatures was first investigated as a reference experiment in the absence of H$_2$O$_2$ (Fig. S2, ESI†). CN$_{600}$ possesses the highest photocatalytic performance in the decomposition of RhB, presumably following the higher light absorption. However, CN$_{600}$ also shows a low photoluminescence intensity (Fig. S3, ESI†), which points to the presence of defects promoting electron localization and thus preventing charge recombination. As a third effect, also the surface adsorption depends on temperature: the absorption capacity of RhB was found to be 6.3% for CN$_{500}$, 7.3% for CN$_{550}$ and 11.2% for
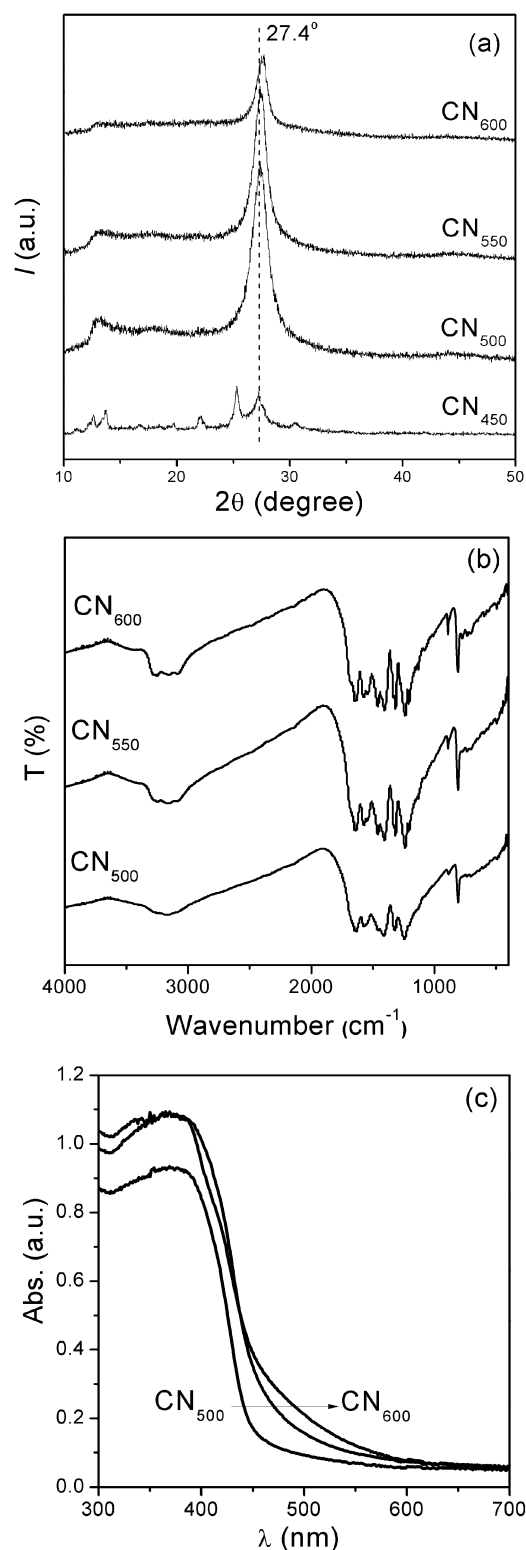

Fig. 1 XRD patterns (a), FT-IR spectrum (b), and diffuse reflectance absorption spectrum (c) of g-C$_3$N$_4$ synthesized at different temperatures.

CN$_{600}$, respectively. Therefore, CN$_{600}$ was applied for the follow-up experiments. For the CN$_{600}$/RhB system, 97% decoloration was obtained under visible light for 200 min in the presence of minor amounts of dissolved dioxygen, while no degradation was observed in the dark (Fig. 2).
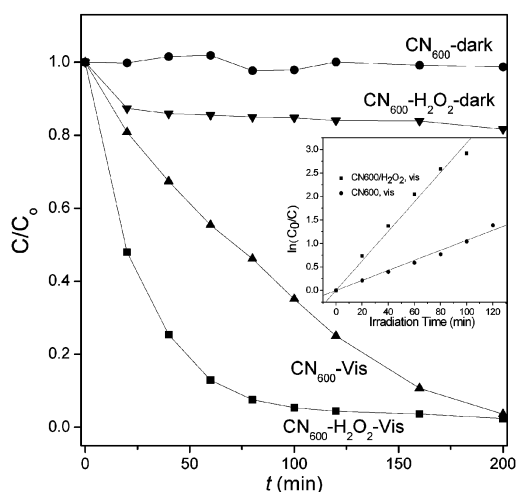
Fig. 2 Visible-light photocatalytic degradation of RhB (10^{-5} M) over CN_{600} with or without H_2O_2 (0.01 M).

Fig. 3 shows that RhB degradation over the g-C_3N_4 catalyst depends systematically on pH and was found to increase with decreasing pH. The adsorption experiments showed that the pH value does not greatly affect the adsorption of RhB on g-C_3N_4 (Table S2, ESI†). It is clear that [H^+] has to promote the rate determining step. It is for instance known that the activation of oxidation occurs *via* an electron transfer cascade known as the "oxygen reduction reaction", ORR. In a first step, the moderate oxidant $^\bullet O_2^-$ is produced by the reaction of dissolved O_2 with a first photoinduced electron. [H^+] is important in the second step, where it helps to transfer a second electron to form H_2O_2 (eqn (1) and (2)).[22] H_2O_2 can then further be activated to the most reactive $^\bullet OH$ by accepting a third photoinduced electron, a key step which g-C_3N_4 is known to be able to perform, due to its band positions (eqn (3)). The $^\bullet OH$ radical is reactive enough to promote the complete mineralization of RhB.
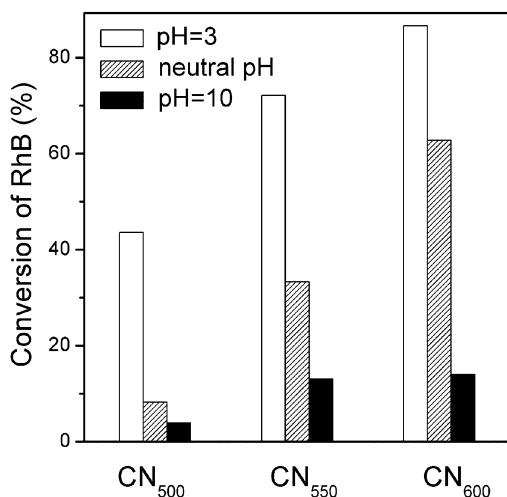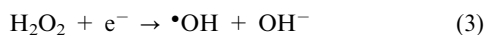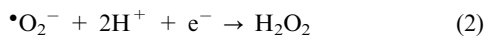
$$O_2 + e^- \rightarrow {}^\bullet O_2^- \tag{1}$$

$$^\bullet O_2^- + 2H^+ + e^- \rightarrow H_2O_2 \tag{2}$$

$$H_2O_2 + e^- \rightarrow {}^\bullet OH + OH^- \tag{3}$$

Fig. 3 Photocatalytic conversion of RhB (10^{-5} M) at different pH values over g-C_3N_4 obtained at different temperatures.

Another option is that in the absence of oxygen, the dye is oxidized directly by the carbon nitride. Here, analogous to the direct photooxidation of alcohols,[23] the photogenerated hole is directly transferred to the dye, which then undergoes follow-up reactions to change its conjugated system. The photochemical electron then has to react with H^+ to liberate hydrogen.

To prove at least the presence of an oxygen-based mechanism and check for the production of H_2O_2, a colorimetric titration method was used under acidic reaction conditions, using the formation of the yellow colored Ti(IV)–H_2O_2 complex.[24] The characteristic absorption peak at $\lambda = 410$ nm (Fig. 4) was found, supporting the production of trace amounts of H_2O_2 (note that the third photoreduction process is significantly faster than the second one). This however does not disprove the coexistence of a direct photooxidation of the dye.

To differentiate more clearly between the two options and to further enhance the photocatalytic oxidation efficiency of the system, the first two photoreduction steps of oxygen can be "short-cutted" by addition of a small amount of H_2O_2 (0.01 M). As expected, the photocatalytic decoloration of RhB was accelerated (95% conversion in 100 min, CN_{600}/RhB/ H_2O_2). The degradation of RhB can be described as a pseudo-first-order reaction. No degradation of RhB was detected without the catalyst but in the presence of H_2O_2 and visible light. These control experiments confirmed that the activation of H_2O_2 was induced by g-C_3N_4 excited with visible light.

Note that for the oxidant-poor CN_{600}/RhB system, the absorption maximum of the degraded solution (λ_{max}) exhibited a marked hypsochromic shift from 554 to 497 nm before complete decolorization occurred at an irradiation time of 200 min (Fig. 5a). This absorption band shift was previously suggested to be induced by the formation of a series of chemically stable intermediates generated in a stepwise manner.[25]

In the CN_{600}/RhB/H_2O_2 system, no obvious absorption band shift was observed, and the main absorbance features in both visible and UV regions were simultaneously diminished with irradiation (Fig. 5b). This suggests that both the dye
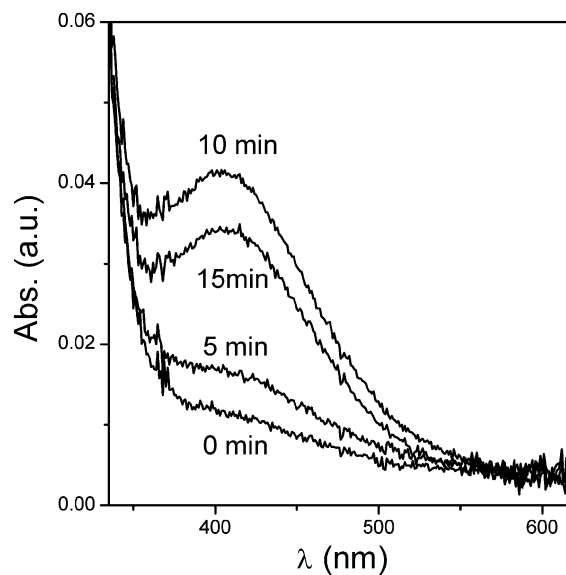

Fig. 4 Absorption spectrum of Ti(IV)–H_2O_2 generated by CN_{600} in HCl solution (pH = 1) under visible light irradiation.
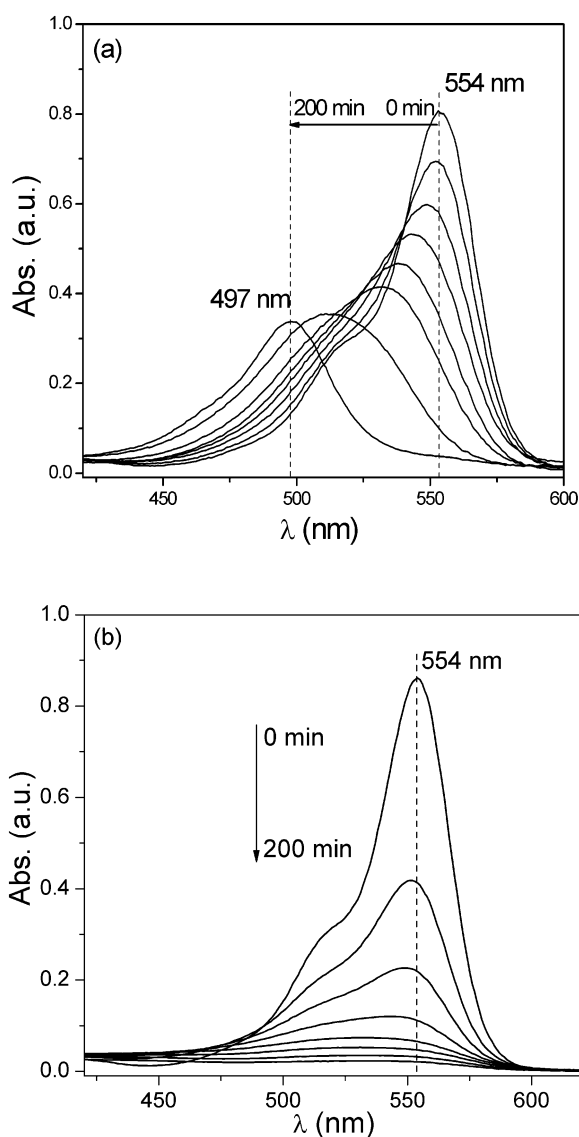
Fig. 5 The temporal absorption spectrum changes of RhB (10^{-5} M) aqueous solution in the presence of CN_{600} under visible light irradiation ($\lambda > 420$ nm), (a) CN_{600}/RhB, (b) CN_{600}/RhB/0.01M H_2O_2 systems, respectively.

chromophores and aromatic rings were oxidized. These results indicate, in our opinion, that indeed both the described reaction channels are active, and their relative importance depends on the oxidant concentration. The combination of g-C_3N_4 and H_2O_2 not only accelerated the decomposition rate of RhB, but also promoted the activation of the oxidant (instead of the direct photooxidation) where the dye molecules are oxidized to a certain deep extent instead of being only decolorized.

It was found that with increasing H_2O_2 concentration from 0.01 M to 0.08 M, k (the pseudo first-order kinetic constant) increased gradually from 0.021 to 0.044 min^{-1} (Fig. S4, ESI†) and then saturated. This means that a small amount of H_2O_2 is able to run the reaction efficiently, while a further increase beyond 0.08 M did not result in a faster reaction. This observation is believed to be related to the fact that excessive

H_2O_2 essentially acts as a self–scavenger for $^\bullet$OH, following eqn (4) and (5).[26]

$$H_2O_2 + {}^\bullet OH \rightarrow {}^\bullet OOH + H_2O \qquad (4)$$

$${}^\bullet OOH + {}^\bullet OH \rightarrow H_2O + O_2 \qquad (5)$$
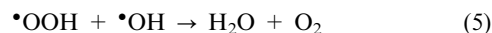
Performing RhB photodegradation at different pH values for the CN_{600}/RhB/H_2O_2 system confirmed that the photodegradation rate under acidic conditions is higher than that under neutral conditions. When the pH value was decreased from 7 to 2, k was increased from 0.044 min^{-1} to 0.0795 min^{-1}. It is noted that, when using HCl as pH regulator, Cl$^-$ ions are able to scavenge $^\bullet$OH in acidic solution. Thus, the photocatalytic activity of carbon nitride is expected to be even more enhanced under other acidic solutions free of Cl$^-$ ions. Not unexpectedly, RhB could be decolorized with H_2O_2 rapidly under basic conditions even without using the catalyst. This can be explained by the existence of HO_2^- (the conjugate base of H_2O_2) in basic media, which is known to be a common discoloration reagent.[27]

3.3. LCMS analysis

LCMS was used to quantify the residual dye and degradation intermediates of RhB in the CN_{600}/H_2O_2 (0.01 M) system, as given in Fig. 6. The corresponding mass peak intensities for RhB and by-products varied gradually with the irradiation time. The LCMS data demonstrated that the peak intensities of consecutive products (at $m/z = 415$, 387, 359 and 331) were first increased and then decreased gradually, indicating that the by-products formed were under those conditions unstable and finally degraded to a large extent. For comparison, the intermediates of RhB degradation in the absence of H_2O_2 were also analyzed (Fig. 7). The rate of decomposition of RhB molecules ($m/z = 443$) was slower, but worth noting are the intermediates having an m/z value of 475 and 419. These can be explained by the direct photooxidization of the nitrogen bound ethyl groups (–C_2H_5) to carboxyl groups (–COOH) in the RhB molecules. These intermediates are less coloured, but relatively stable and as a result, the rate of degradation of RhB was inhibited to a certain degree. The de-ethylated intermediates
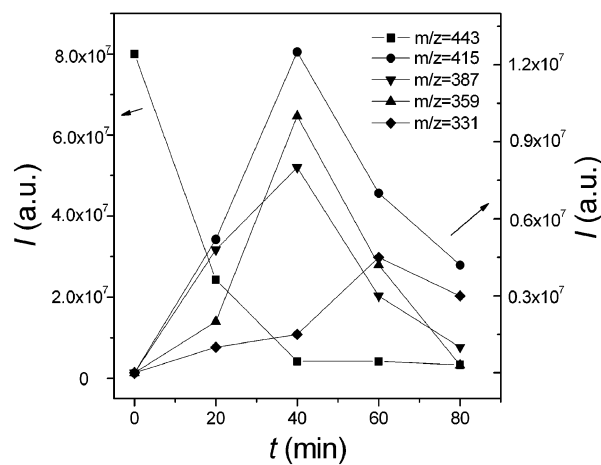

Fig. 6 Mass spectrum intensity changes of the main peaks appearing at different retention times in the photocatalytic degradation process over CN_{600}/H_2O_2 (0.01 M) under visible light illumination.
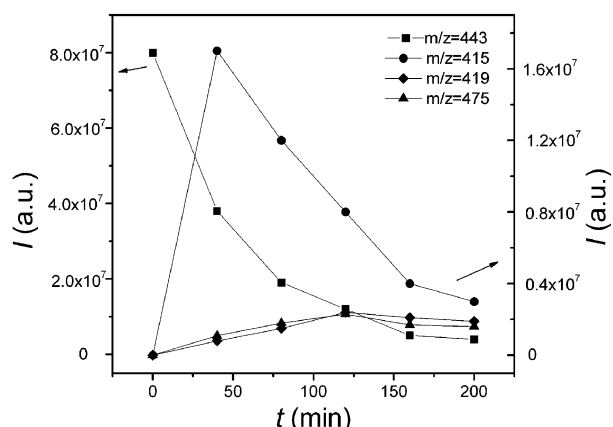
Fig. 7 Mass spectrum intensity changes of the main peaks appearing at different retention times in the photocatalytic degradation process over CN_{600} under visible light illumination, in the absence of H_2O_2.

were also detected in the CN_{600}/H_2O_2 system, however with the cleavage of the xanthene conjugated rings occurring to a more significant extent. We rationalized the molecular structure of various intermediate degradation products (Fig. S7, ESI†). All these data support the mechanism discussed above with its coexistence of the two possible reaction channels.

3.4. Miscellaneous experiment

To study the oxidative reaction mechanism, photocatalytic experiments were performed under different atmospheres. It was observed that the degradation rate of RhB was depressed under an N_2 atmosphere but improved when conducted in the presence of bubbling O_2, as compared with the reaction under air equilibrium (no gas flow) (Fig. 8a). This implied that the dissolved O_2 in the solution acted as e_{cb}^- trapper, leading to the generation of active oxygen species $^\bullet O_2^-/^\bullet OOH$. The generation of active oxygen species $^\bullet O_2^-/^\bullet OOH$ was confirmed by the additional ESR/DMPO experiments (Fig. 9b). DMPO/$^\bullet O_2^-$ adducts clearly appeared when the CN_{600}/RhB system was exposed to visible light irradiation. However, no detectable $^\bullet OH$ signals were found in experiments carried out under darkness or visible light irradiation. Addition of benzoquinone (BQ, 10 mM), a very efficient trap of $^\bullet O_2^-$,[28] hindered the decomposition of RhB almost completely. These results indicate that $^\bullet O_2^-$ was the major oxidation species during degradation of RhB in the CN_{600}/RhB system under neutral conditions without the addition of H_2O_2. That is to say, the cleavage of the RhB chromophore structure is mainly attributed to attack of dye by $^\bullet O_2^-/^\bullet OOH$ ions. Note that $^\bullet O_2^-/$ $^\bullet OOH$ are relatively mild oxidants, offering an explanation for the observed absorption band shift related to partial oxidation instead of mineralization (Fig. 5a). It was also observed that the degradation was inhibited by the addition of isopropanol (an efficient trap of free $^\bullet OH$), which is significant but does not lead to complete quenching of the reaction (Fig. 8a). This result, together with the above experimental effect of BQ addition, demonstrated the fact that $^\bullet OH$ is involved but not exclusively and that the major oxidation species is $^\bullet O_2^-$ in RhB degradation without H_2O_2.
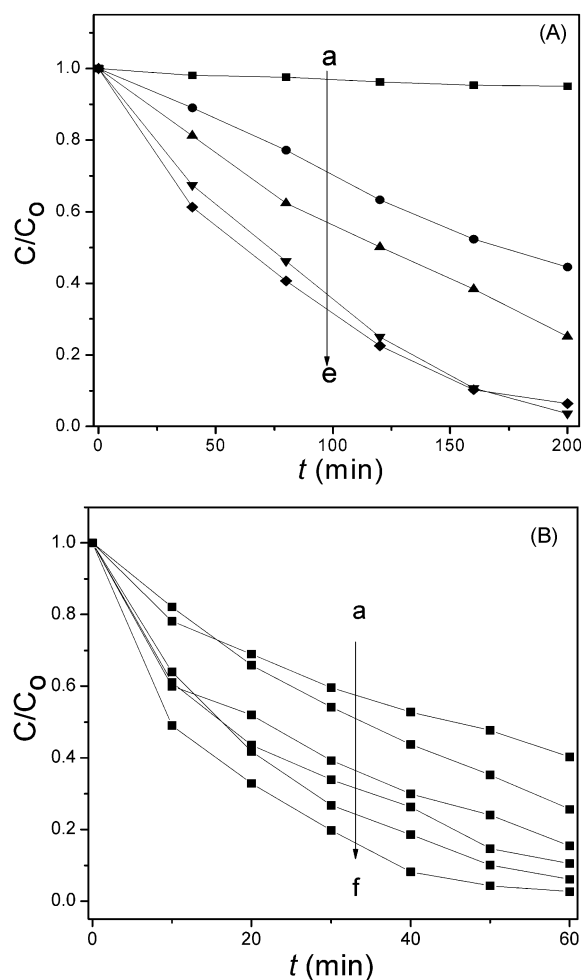

Fig. 8 Time-dependent degradation of RhB by the effect of oxygen and other additives: (A) CN_{600}: (a) 10 mM BQ; (b) N_2-bubbling systems; (c) 10 vol% isopropanol; (d) no addition; (e) O_2-bubbling systems. (B) CN_{600}/H_2O_2 (0.08 M): (a) 10 mM BQ; (b) 10 vol% isopropanol; (c) N_2-bubbling systems; (d) 100 mM N_3^-; (e) no addition; (f) O_2-bubbling systems.

In the case of $CN_{600}/RhB/H_2O_2$ system (Fig. 8b), the addition of both BQ (10 mM) and isopropanol (10 vol%) led to suppression of the degradation rate of RhB, revealing the direct involvement of $^\bullet O_2^-$ and $^\bullet OH$ radicals in the photochemical reaction scheme with H_2O_2, as confirmed by the ESR experiments (Fig. 9).

To further confirm the active species in the H_2O_2-assisted system, ESR/DMPO or TEMPO spin trapping experiments were carried out. Before irradiation, weak characteristic peaks of DMPO/$^\bullet OH$ signals with an intensity ratio of 1 : 2 : 2 : 1 could be observed for the CN_{600}/H_2O_2/DMPO system which may be resulted from the thermal decomposition of H_2O_2 itself (Fig. 9a).[29,30] This is consistent with the fact that a small fraction of RhB was degraded in the $CN_{600}/RhB/H_2O_2$ system in the dark, but with modest performance. Under visible light irradiation, the intensity of DMPO/$^\bullet OH$ signals in the $CN_{600}/$ H_2O_2 system increased largely, indicating that the photogenerated electrons can drive the decomposition of H_2O_2 to produce $^\bullet OH$.

The potential involvement of other radicals in the photocatalytic CN_{600} and CN_{600}/H_2O_2 systems, such as singlet

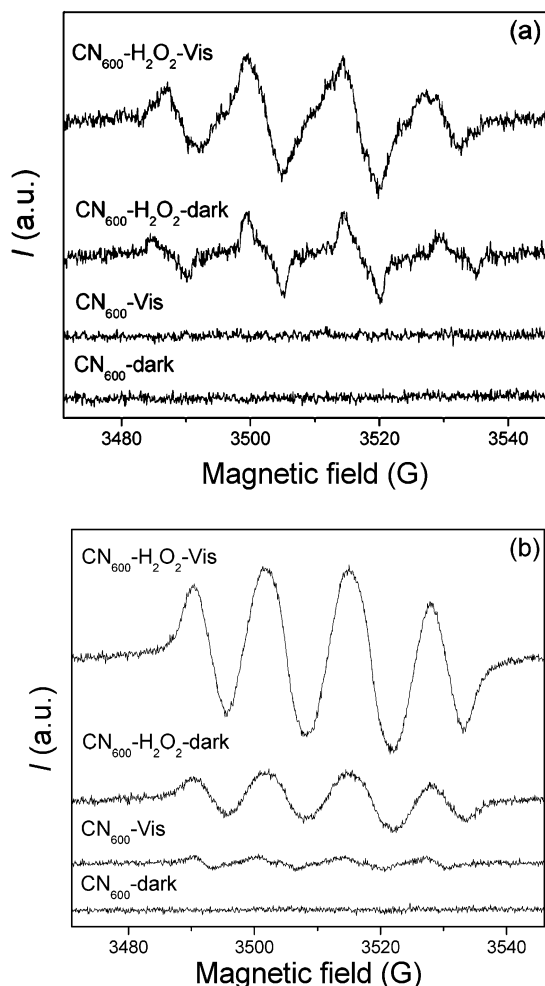Fig. 9 ESR spectra of DMPO–•OH and DMPO–•O_2^-/•OOH adducts in the systems of CN_{600}/DMPO and CN_{600}/DMPO/H_2O_2 (0.08 M) before and after visible light irradiation.

Fig. 10 ESR spectra of TEMPO–$^1O_2$ adducts in the systems of CN_{600}/H_2O_2 (0.08 M) and CN_{600} before and after visible light irradiation.

presence of H_2O_2 (0.08 M). The removal of TOC of RhB in the CN_{600}/RhB/H_2O_2 system was about 61.3% after 5 h of irradiation, i.e. this is the extent of total mineralization. The TOC then was observed to continue to decline afterwards. The consumption of H_2O_2 throughout the reaction was small, retaining 89% of the original concentration after 300 min, thus allowing application of even much smaller starting concentrations. Note that in the H_2O_2-free system, 51% of RhB was decolorized but with a mineralization ratio of only ca. 3.4% after being irradiated for 5 h, indicating that most of RhB is bleached instead of being mineralized. The acceleration of RhB mineralization to CO_2 can be therefore attributed to the generation of the more active oxidation agent •OH by the activation of H_2O_2 with g-C_3N_4.

3.6. Stability evaluation

Bleaching experiments were repeated five times after re-isolation of the catalyst, with no apparent decrease in photocatalytic
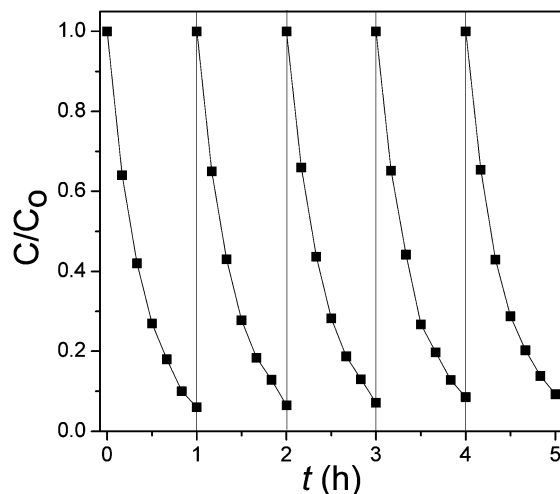
Fig. 11 The cycling runs of the degradation of RhB (10^{-5} M) in the CN_{600}/H_2O_2 (0.08 M) system under visible light irradiation.

oxygen $^1O_2$, was also investigated by ESR using the spin trapping TEMPO (Fig. 10). In these systems, the intensity of TEMPO• signals increased after being illuminated with visible light for 15 min, supporting the generation of singlet oxygen with the superoxide radical ($2•O_2^- + 2H^+ \rightarrow {}^1O_2 + H_2O_2$). However, when H_2O_2 was added, the intensity of TEMPO• signals were lower than that without H_2O_2. This is usually due to the fact that the generation of larger amounts of other radicals inhibits the production of $^1O_2$. Therefore N_3^- was added as a quencher for singlet oxygen to the reaction system, and the addition of N_3^- didn't influence the photocatalytic behavior of CN_{600}/H_2O_2 too much (Fig. 8b). This result suggests that $^1O_2$ as a species can be excluded to be responsible for the photodegradation of RhB. However, N_3^- is also an effective scavenger of •OH, and the negligible influence of N_3^- on the degradation rate of RhB could be attributed to the oxidation of N_3^- to radical •N_3, which is a rather active oxidant and can react with RhB.

3.5. Mineralization investigation

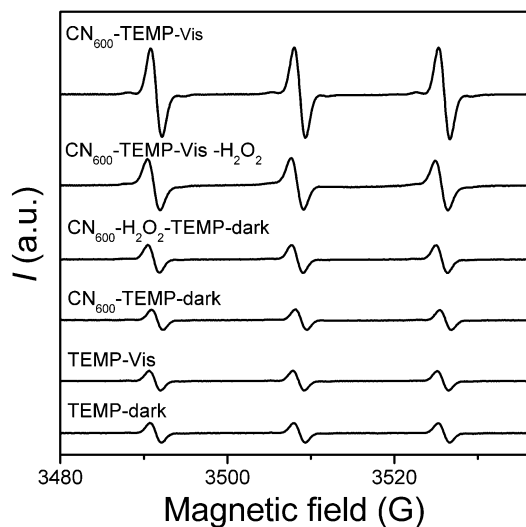Total organic carbon (TOC) experiments were carried out to evaluate the mineralization ratio of RhB by g-C_3N_4 in the

This journal is © the Owner Societies 2012

Phys. Chem. Chem. Phys., 2012, **14**, 1455–1462 | 1461

activity (Fig. 11). In addition, there is no measurable alteration in surface and local X-ray structures of the sample before and after the reactions, as reflected by XRD and FTIR measurements (Fig. S7, ESI†). These results demonstrate that the presented g-C$_3$N$_4$ photocatalyst was stable under the experimental reaction conditions employed here.

In addition, other organic pollutants including methylene blue (MB) and Congo red (CR) were tested and also found to be effectively degraded by g-C$_3$N$_4$ when treated in the presence of H$_2$O$_2$ (Table S4, ESI†). It was found that when RhB, MB or CR was used as a model compound to examine photocatalyst activity, the degradation rate in the presence of H$_2$O$_2$ is in all cases higher than without. The presented results indicate that different type of dyes can be effectively degraded, and the metal-free photocatalysis system can in principle be extended to many stable organic pollutants.

4. Conclusions

Graphitic carbon nitride polymers have been synthesized by a thermal-induced polymerization process, using a simple nitrogen-containing organic compound, dicyandiamide, as a precursor. The obtained g-C$_3$N$_4$ can effectively activate H$_2$O$_2$ under visible light irradiation to generate strong hydroxyl radicals •OH, which are able to mineralize most organics in water. This photocatalytic process avoids the employment of any metal derivatives, and the catalyst was found to be stable and reusable, creating the promise of easily-available carbon nitride materials for environmental applications.

Acknowledgements

Notes and references

1 C. L. Wu, H. Shemer, G. Karl and J. Linden, *J. Agric. Food Chem.*, 2007, **55**, 4095.
2 For examples, see: (*a*) J. H. Ma, W. J. Song, C. C. Chen and J. C. Zhao, *Environ. Sci. Technol.*, 2005, **39**, 5810; (*b*) X. P. Zhang, D. L. Zhang, D. H. Busch and R. V. Eldik, *J. Chem. Soc., Dalton Trans.*, 1999, 2751; (*c*) C. Y. Sun, C. C. Chen, W. H. Ma and J. C. Zhao, *Phys. Chem. Chem. Phys.*, 2011, **13**, 1957.
3 X. Zhao and Y. F. Zhu, *Environ. Sci. Technol.*, 2006, **40**, 3367.
4 For examples, see: (*a*) L. M. Shen, N. Z. Bao, Y. Q. Zheng, A. Gupta, T. C. An and K. Yanagisawa, *J. Phys. Chem. C*, 2008, **112**, 8809; (*b*) J. C. Zhao, K. Q. Wu, T. X. Wu, H. Hidaka and N. Serpone, *J. Chem. Soc., Faraday Trans.*, 1998, **94**(5), 673;

(*c*) X. Z. Li, G. M. Liu and J. C. Zhao, *New J. Chem.*, 1999, **23**, 1193; (*d*) V. J. O. Vilar, A. I. E. Gomes, V. M. Ramos, M. I. Maldonado and R. A. R. Boaventura, *Photochem. Photobiol. Sci.*, 2009, **8**, 691; (*e*) J. H. Huang, Y. J. Cui and X. C. Wang, *Environ. Sci. Technol.*, 2010, **44**, 3500.
5 J. Wahlen, D. E. De Vos and P. A. Jacobs, *Org. Lett.*, 2003, **5**, 1777.
6 Y. L. Nie, C. Hu, J. H. Qu, L. Zhou and X. X. Hu, *Environ. Sci. Technol.*, 2007, **41**, 4715.
7 F. Martinez, J. A. Melero, J. A. Botas and R. Molina, *Ind. Eng. Chem. Res.*, 2007, **46**, 4396.
8 R. Su, J. Sun, Y. P. Sun, K. J. Deng, D. M. Cha and D. Y. Wang, *Chemosphere*, 2009, **77**, 1146.
9 S. Caudo, C. Genovese, S. Perathoner and G. Centi, *Microporous Mesoporous Mater.*, 2008, **107**, 46.
10 A. D. Bokare and W. Choi, *Environ. Sci. Technol.*, 2010, **44**, 7232.
11 Y. W. Ma, S. J. Jiang, G. Q. Jian, H. S. Tao, L. S. Yu, X. B. Wang, X. Z. Wang, J. M. Zhu, Z. Hu and Y. Chen, *Energy Environ. Sci.*, 2009, **2**, 224.
12 For examples, see: (*a*) J. S. Zhang, X. F. Chen, K. Takanabe, K. Meaeda, K. Domen, J. D. Epping, X. Z. Fu, M. Antonietti and X. C. Wang, *Angew. Chem., Int. Ed.*, 2010, **49**, 441; (*b*) J. S. Zhang, J. H. Sun, K. Maeda, K. Domen, P. Liu, M. Antonietti, X. Z. Fu and X. C. Wang, *Energy Environ. Sci.*, 2011, **4**, 675.
13 For examples, see: (*a*) X. C. Wang, K. Maeda, A. Thomas, K. Takanabe, G. Xin, K. Domen and M. Antonietti, *Nat. Mater.*, 2009, **8**, 76; (*b*) K. Maeda, X. C. Wang, Y. Nishihara, D. Lu, M. Antonietti and K. Domen, *J. Phys. Chem. C*, 2009, **113**, 4940; (*c*) J. S. Zhang, M. Grzelczak, Y. D. Hou, K. Maeda, K. Domen, X. Z. Fu, M. Antonietti and X. C. Wang, *Chem. Sci.*, 2012, DOI: 10.1039/c1sc00644d.
14 X. F. Chen, J. S. Zhang, X. Z. Fu, M. Antonietti and X. C. Wang, *J. Am. Chem. Soc.*, 2009, **131**, 11658.
15 X. C. Wang, X. F. Chen, A. Thomas, X. Z. Fu and M. Antonietti, *Adv. Mater.*, 2009, **21**, 1609.
16 S. C. Yan, Z. S. Li and Z. G. Zou, *Langmuir*, 2009, **25**, 10397.
17 A. Thomas, A. Ficher, F. Goettmann, M. Antonietti, J. Muller and J. M. Carlsson, *J. Mater. Chem.*, 2008, **18**, 4893.
18 Z. X. Ding, X. F. Chen, M. Antonietti and X. C. Wang, *ChemSusChem*, 2011, **4**, 274.
19 Q. X. Guo, Y. Xie, X. J. Wang, S. C. Lv, T. Hou and X. M. Liu, *J. Phys. Chem. Lett.*, 2003, **380**, 84.
20 B. V. Lotsch and W. Schnick, *Chem. Mater.*, 2006, **18**, 1891.
21 S. Hwang, S. Lee and J. S. Yu, *Appl. Surf. Sci.*, 2007, **252**, 5656.
22 L. M. Yang, L. E. Yu and M. B. Ray, *Environ. Sci. Technol.*, 2009, **43**, 460.
23 F. Z. Su, S. C. Mathew, G. Lipner, X. Z. Fu, M. Antonietti, S. Blechert and X. C. Wang, *J. Am. Chem. Soc.*, 2010, **132**, 116299.
24 G. Eisenberg, *Ind. Eng. Chem., Anal. Ed.*, 1943, **15**, 327.
25 T. X. Wu, G. M. Liu and J. C. Zhao, *J. Phys. Chem. B*, 1998, **102**, 5845.
26 T. Watanabe, T. Takizawa and K. Honda, *J. Phys. Chem.*, 1977, **81**, 1845.
27 A. Gartner and G. Gellerstedt, *J. Pulp Pap. Sci.*, 2001, **27**, 240.
28 E. Baciocchi, T. D. Giacco, F. Elisei, M. F. Gerini, M. Guerra, A. Lapi and P. Liberali, *J. Am. Chem. Soc.*, 2003, **125**, 16444.
29 M. Ravera, A. Buico, F. Gosetti, C. Cassino, D. Musso and D. Osella, *Chemosphere*, 2009, **74**, 1309.
30 Y. V. Haglili, L. Weiner, V. Brumfeld, A. Brandis, Y. Salomon, B. Mcllroy, B. C. Wilson, A. Pawlak, M. Rozanowska, T. Sarna and A. Scherz, *J. Am. Chem. Soc.*, 2005, **127**, 6487.